doi:10.1016/S0022-2836(02)01132-4 available online at http://www.idealibrary.com on IDEAL® J. Mol. Biol. (2002) 324, 755–762

JMB

Observation of Additional Calcium Ion in the Crystal Structure of the Triple Mutant K56,120,121M of Bovine Pancreatic Phospholipase A_2

V. Rajakannan[1], M. Yogavel[1], Ming-Jye Poi[2], A. Arockia Jeyaprakash[3] J. Jeyakanthan[3], D. Velmurugan[1], Ming-Daw Tsai[2] and K. Sekar[4,5]*

[1]*Department of Crystallography and Biophysics University of Madras, Guindy Campus, Chennai 600 025 India*

[2]*Departments of Chemistry and Biochemistry, and the Ohio State Biochemistry Program Ohio State University Columbus, OH 43210, USA*

[3]*Molecular Biophysics Unit Indian Institute of Science Bangalore 560 012, India*

[4]*Bioinformatics Centre, Indian Institute of Science, Raman Building, Bangalore 560 012 India*

[5]*Supercomputer Education and Research Centre, Indian Institute of Science, Bangalore 560 012, India*

**Corresponding author*

Phospholipase A_2 catalyses hydrolysis of the ester bond at the C2 position of 3-*sn*-phosphoglycerides. Here we report the 1.9 Å resolution crystal structure of the triple mutant K56,120,121M of bovine pancreatic phospholipase A_2. The structure was solved by molecular replacement method using the orthorhombic form of the recombinant phospholipase A_2. The final protein model contains all the 123 amino acid residues, two calcium ions, 125 water molecules and one 2-methyl-2-4-pentanediol molecule. The model has been refined to a crystallographic *R*-factor of 19.6% (R_{free} of 25.9%) for all data between 14.2 Å and 1.9 Å. The residues 62–66, which are in a surface loop, are always disordered in the structures of bovine pancreatic phospholipase A_2 and its mutants. It is interesting to note that the residues 62–66 in the present structure is ordered and the conformation varies substantially from those in the previously published structures of this enzyme. An unexpected and interesting observation in the present structure is that, in addition to the functionally important calcium ion in the active site, one more calcium ion is found near the N terminus. Detailed structural analyses suggest that binding of the second calcium ion could be responsible for the conformational change and the ordering of the surface loop. Furthermore, the results suggest a structural reciprocity between the k^*_{cat} allosteric site and surface loop at the i-face, which represents a newly identified structural property of secreted phospholipase A_2.

© 2002 Elsevier Science Ltd. All rights reserved

Keywords: phospholipase A_2; crystal structure; calcium ion; phospholipid binding; surface loop residues

Introduction

Phospholipase A_2 (PLA2) catalyzes hydrolysis of the fatty acid ester bond at the position 2 of 1,2-diacyl-3-*sn*-glycerophospholipids.[1] The enzyme is found both inside and outside the cell. For example, extra cellular phospholipase A_2 is found in mammalian pancreas and in venoms (for example snake and bee). This enzyme has been studied extensively in the past few decades. A comprehensive review on the structure–function relationship of PLA2 has been published recently.[2] Despite major progresses made in recently years as described in this review, some of the issues related to the structure–function relationship of PLA2 remain to be resolved.

One of such issues involves the structural and functional role of the "surface loop", consisting of residues 62–66 (or more inclusively residues 60–70) in pancreatic PLA2. The primary structures of the PLA2 enzyme from bovine and porcine pancreas share more than 85% sequence identity. In addition, the residues 59–70 are identical in sequence except the residues at position 63 (Phe in porcine and Val in bovine). However, residues 62–66 have been found to be disordered in all of the structures of bovine pancreatic PLA2 and its mutants,[3–6] while they exist in a well ordered conformation in the porcine enzyme.[7]

The difference in the conformation and dynamics of the surface loop residues could be related to binding of a second calcium ion, though

Abbreviations used: PLA2, phospholipase A_2.

E-mail address of the corresponding author: sekar@physics.iisc.ernet.in

 © 2002 Elsevier Science Ltd. All rights reserved

there has been no direct evidence for this correlation. While calcium ion in the active site is an essential cofactor for both bovine and porcine enzymes, an additional calcium ion has been reported in porcine PLA2 enzyme[7–8] but not in bovine pancreatic PLA2. The ligands of the second calcium ion in the porcine enzyme include residues at or near the surface loop.

Here, the paper describes a novel finding that the crystal structure of a triple mutant of bovine pancreatic PLA2 displays a ordered surface loop structure, and also binds a second calcium ion, which provide an evidence for the correlation between these two properties. Furthermore, the triple mutant displaying this property is K56,120,121M, which involves residues at the "k^*_{cat} allosteric site"[2] distant from the surface loop residues. Since the surface loop is part of the i-face, our results also provide evidence for structural relationship between residues at these two sites.

Results and Discussion

Quality of the triple mutant model

The final refined model consists of 954 non-hydrogen atoms from 123 amino acid residues, 125 water molecules, two calcium ions and one 2-methyl-2,4-pentanediol (MPD) molecule. The crystallographic *R*-factor for the final refined model is 19.6% (R_{free} = 25.9%) for all the reflections in the resolution range 14.2–1.9 Å. The root mean square deviations (rmsd) from ideal geometry for the bond length, bond angle and dihedral angle are given in Table 1. The coordinate error estimated using σ(*A*) method is 0.13 Å. The program PROCHECK[9] was used to assess the quality of the final model. More than 89% of the residues are in the most favored regions of the Ramachandran plot and no residue is observed in the disallowed region. A total of 125 water molecules were located and most of them are in the first hydration shell, while 20 are in the second hydration shell. Of the first hydration shell water molecules, 60 water molecules are hydrogen bonded to the peptide backbone atoms while the remaining are hydrogen-bonded to the side-chain atoms. The first hydration shell water molecules make 106 and 110 hydrogen bonds (<3.6 Å) with the polar atoms of the main-chain and side-chain, respectively, of the protein molecule.

Table 1. Crystal and other relevant geometrical parameters of the triple mutant K56,120,121M

Unit cell parameters	
a (Å)	39.10
b (Å)	24.35
c (Å)	67.11
β (deg.)	102.2
Space group	*P*2
Resolution range (Å)	14.2–1.9
Total number of observations	40,817
Unique reflections	8880
R_{merge} (%)	7.5
Cumulative completeness (%) at 1.9 Å	88.3
R_{work} (%) for 8033 reflections	19.6
R_{free} (%) for 949 reflections	25.9
Z	2
RMS deviation from ideal bond lengths (Å)	0.011
RMS deviation from ideal bond angles (deg.)	2.1
RMS deviation from ideal dihedral (deg.)	22.9
RMS deviation from ideal improper (deg.)	2.56
Average atomic temperature factors of the refined model (Å^2)	
Main-chain atoms	15.7
Side-chain atoms	18.8
Water molecules	33.1
Calcium ion (Ca^{2+})	14.1
MPD molecule	40.5

$R_{merge} = \sum_{hkl} |I - \langle I \rangle| / \sum I$, where *I* is the observed intensity and $\langle I \rangle$ is the average intensity from observations of symmetry related reflections, respectively.

The electron density, in general, is very clear for all the regions of the protein model. It is important to note that the surface loop containing 11 residues (residues 60–70) has clear electron density (Figure 1) except the end atoms of the side-chain, Leu 64. Most interestingly the loop adopts a different conformation (see discussion below) compared to the other forms of recombinant bovine PLA2 structures. The superposition of the triple mutant structure to the structures of the trigonal[5] and orthorhombic[10] forms of the recombinant enzyme indicated that the overall fold is similar except the surface loop. The backbone atoms (492 atoms) superimpose on the trigonal and orthorhombic enzymes with a rmsd of 1.21 Å and 1.31 Å, respectively. The largest deviations are seen in the surface loop and at the C-terminal region (residues 116–123). The rmsd values are reduced to 0.74 Å and 0.80 Å, respectively, if the largest deviating residues are omitted from the calculation.

A secondary calcium ion is present in the triple mutant structure

As stated above, there is a huge peak (>6σ) near the N-terminal region. An additional calcium ion has been observed in the porcine PLA2 enzyme in the same place where a strong peak is seen in the present study.[7,8] The backbone atoms of the present triple mutant structure (the residues 60–70 and the C-terminal region 116–123 are not included) superposes very well with the porcine PLA2 structure[7] (PDB-id code: 1P2P) with an rmsd of 0.89 Å. The primary and the secondary calcium ions of the porcine PLA2 enzyme are 0.91 Å and 0.76 Å away from the primary calcium ion and the strong peak, respectively, observed in the present structure. Similarly, the distances are 0.51 Å and 0.51 Å, respectively, upon superposition with the F63V single mutant (PDB-id code: 2PHI) porcine PLA2 enzyme.[8] These comparisons provided a lead that the strong peak corresponds to a metal ion.

Before proceeding further, it was important to establish that the observed density corresponds to

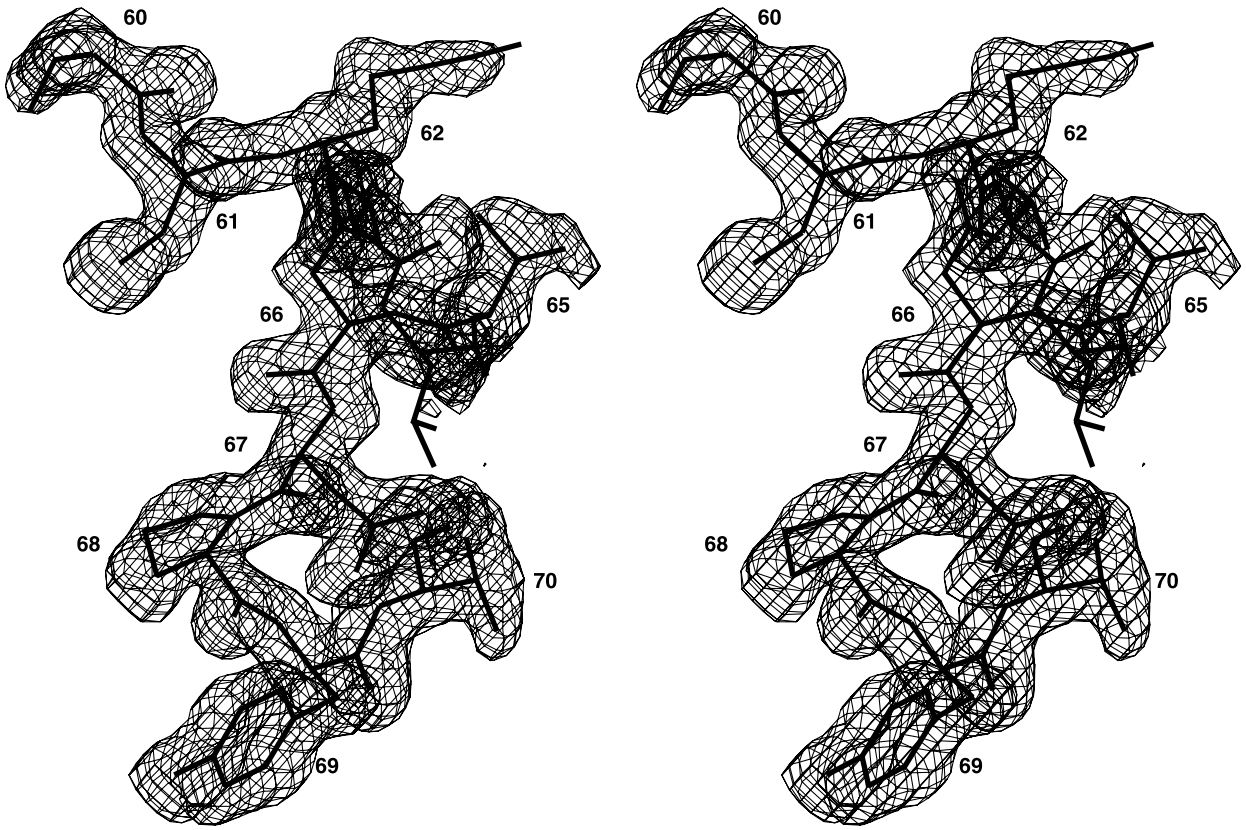

Figure 1. A stereo-view of the omit electron density map showing the ordered surface loop residues 60–70 in the present triple mutant, contoured at 1.0σ level. The electron density is very clear, except the end atoms of the side-chain Leu64.

a calcium ion instead of a chloride ion, since $CaCl_2$ was used in the crystallization buffer. Towards this effort, a systematic study was carried out by analyzing all calcium and chloride ion containing protein structures in the resolution range 1.89–1.91 Å in the Protein Data Bank.[11] Of the 191 structures analyzed, the average chloride–ligand distances were 3.16 Å and 3.26 Å (minimum and maximum, respectively). Similar calculation with the calcium ion revealed the distances of 2.50 Å and 2.52 Å, respectively. In the present triple mutant structure, the corresponding values were 2.31 Å and 2.60 Å, respectively. On the basis of the distances, we concluded that the strong peak corresponds to a calcium ion. In addition, the electron density is very clear for all coordinated ligands for this calcium ion (Figure 2). In the porcine PLA2 crystal structure[7] (PDB-id code: 1P2P), the second calcium ion has only four ligands (two ligands from the reference protein molecule and the remaining two from the same atoms of the crystallographic symmetry related molecule) with an average distance of 2.52 Å. The two reference protein ligands are from the backbone carbonyl oxygen of Ser72 and the $O^{\varepsilon 1}$ atom of Glu92. In another crystal structure[8] (PDB-id code: 2PHI), the second calcium ion has six ligands, three from the reference protein molecule (the $O^{\varepsilon 1}$ atom of Glu71, the backbone oxygen atom of Ser72, and the $O^{\varepsilon 1}$ of Glu92), the other three from the same atoms of the molecule generated by the non-crystallographic 2-fold axis. The average metal–ligand distance is 2.43 Å. In both structures, the second calcium ion is on the 2-fold axis and stabilizes the interaction between two neighboring molecules in the crystal structure. It is important to note that no water molecules are found in the second calcium ion coordination in these structures. However, in the triple mutant structure, the secondary calcium ion has six ligands, including three protein atoms and three water molecules. The protein ligands are (1) the side-chain atom $O^{\delta 1}$ of Asn71, (2) the backbone carbonyl oxygen of Asn72, and (3) the side-chain atom $O^{\varepsilon 2}$ of Glu92. The calcium–ligand coordination distances range from 2.31 Å to 2.60 Å with an average distance of 2.43 Å. This average distance agrees well with the average distances observed in the second calcium site of porcine PLA2 structures.

Comparison of the secondary Ca^{2+} site in porcine and bovine structures

Early biochemical studies suggested the presence of an extra calcium ion near the N-terminal Ala1 of porcine pancreatic PLA2.[12,13] Later, site-directed mutagenesis studies were performed to identify the acidic amino acid residues

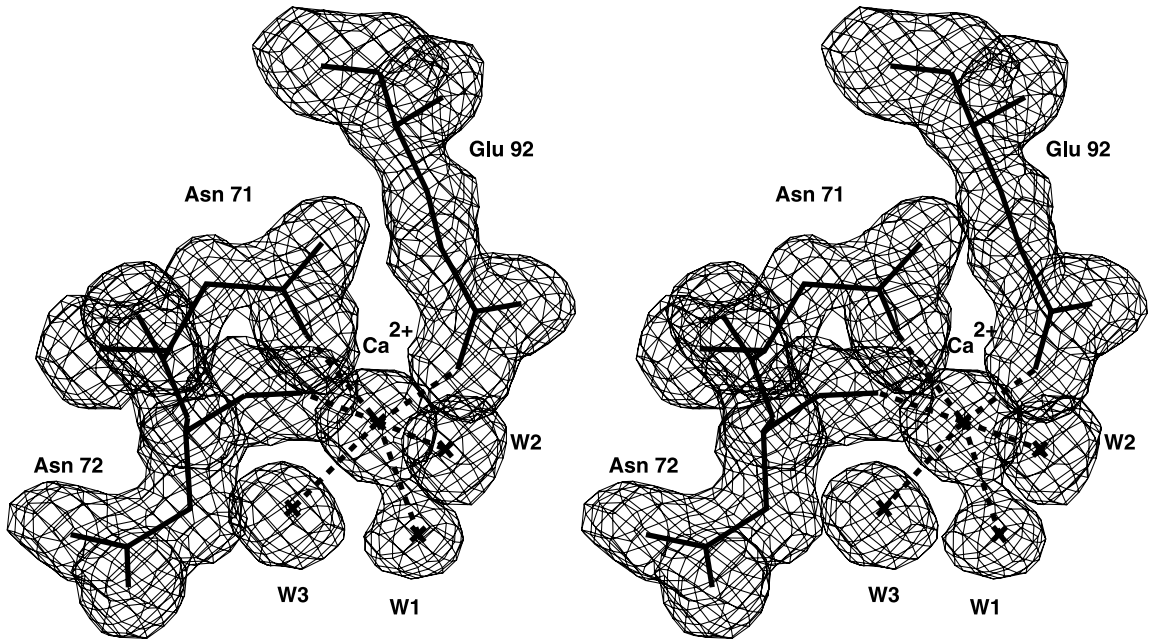

Figure 2. A stereo-view of the omit electron density map showing the second calcium ion and its liganded atoms. Contours are shown at 1.2σ level.

involved in liganding the second calcium ion.[14] From the studies on the three single mutants (D66N, E71N and E92Q), it was concluded that Glu92 was not important for binding the second calcium ion. However, Glu71 and to a lesser extent Asp66 were found both directly involved in the low affinity calcium binding. It has also been suggested that the secondary calcium ion at this site in the bovine pancreatic PLA2 is not possible because of the replacement of Glu at position 71 by Asn.[15] Our present X-ray crystallographic results on the triple mutant differ from previous structures in the following aspects: the residue Asp66 is far away (7.63 Å) from the second calcium ion binding site. The alpha carbon distances of Asp66 to Asn71, Asn72 and Glu92 are 5.3 Å, 8.7 Å and 8.2 Å, respectively. Also the distances between the side-chain carboxylate oxygen atoms ($O^{\delta 1}$ and $O^{\delta 2}$) of Asp 66 and the second calcium ion are 5.65 Å and 7.32 Å, respectively, indicating the absence of this residue in the calcium coordination.

The functional role of the second calcium ion is not clear. However, it could affect interfacial binding by changing the dynamics of the surface loop, as described in the following section.

Ordered surface loop

The residues 62–66 in the surface loop are always found to be disordered in the recombinant bovine pancreatic phospholipase A_2 and its mutant structures studied so far.[5,16] In the present triple mutant, the electron density for these residues (62–66) is very clear (Figure 1). The superposition of the surface loop residues with the corresponding residues in the orthorhombic form is shown in Figure 3. It is clear that the conformation of the surface loop in the triple mutant is different from that in the orthorhombic form. In the orthorhombic form, the side-chain atom $O^{\delta 1}$ of the residue Asn71 is involved in hydrogen bonding with both carboxylate oxygen atoms of Asp66 which, in turn, form hydrogen bonds with the water molecules. Further, these water molecules are hydrogen bonded with the backbone carbonyl oxygen atoms of Leu64 and Val65 (Figure 4(a)). These water-mediated hydrogen bonds seem to dictate the surface loop conformation. In the present structure (Figure 4(b)), the side-chain atoms $O^{\delta 1}$ and $N^{\delta 2}$ of the residue Asn71 are swapped such that one of the atoms ($O^{\delta 1}$) provides coordination to the second calcium ion. In addition, the side-chain conformation of Asp66 is also changed. Consequently, the hydrogen-bonding network is disrupted, which in turn results in a different surface loop conformation. Therefore, the conformational change of Asn71 induced by the secondary calcium ion may be responsible for the alternate surface loop conformation and ordering of the loop. Specifically, the conformational change of the surface loop could bring Asn71 into the direct vicinity to provide possible coordination to the secondary calcium ion. These results support the possible connection between the conformation and dynamics of the surface loop and the binding of second calcium ion.

Structural reciprocity between the k^*_{cat} allosteric site and the i-face

The lysine residues 53, 56, 120 and 121 have been demonstrated to be involved in substrate binding

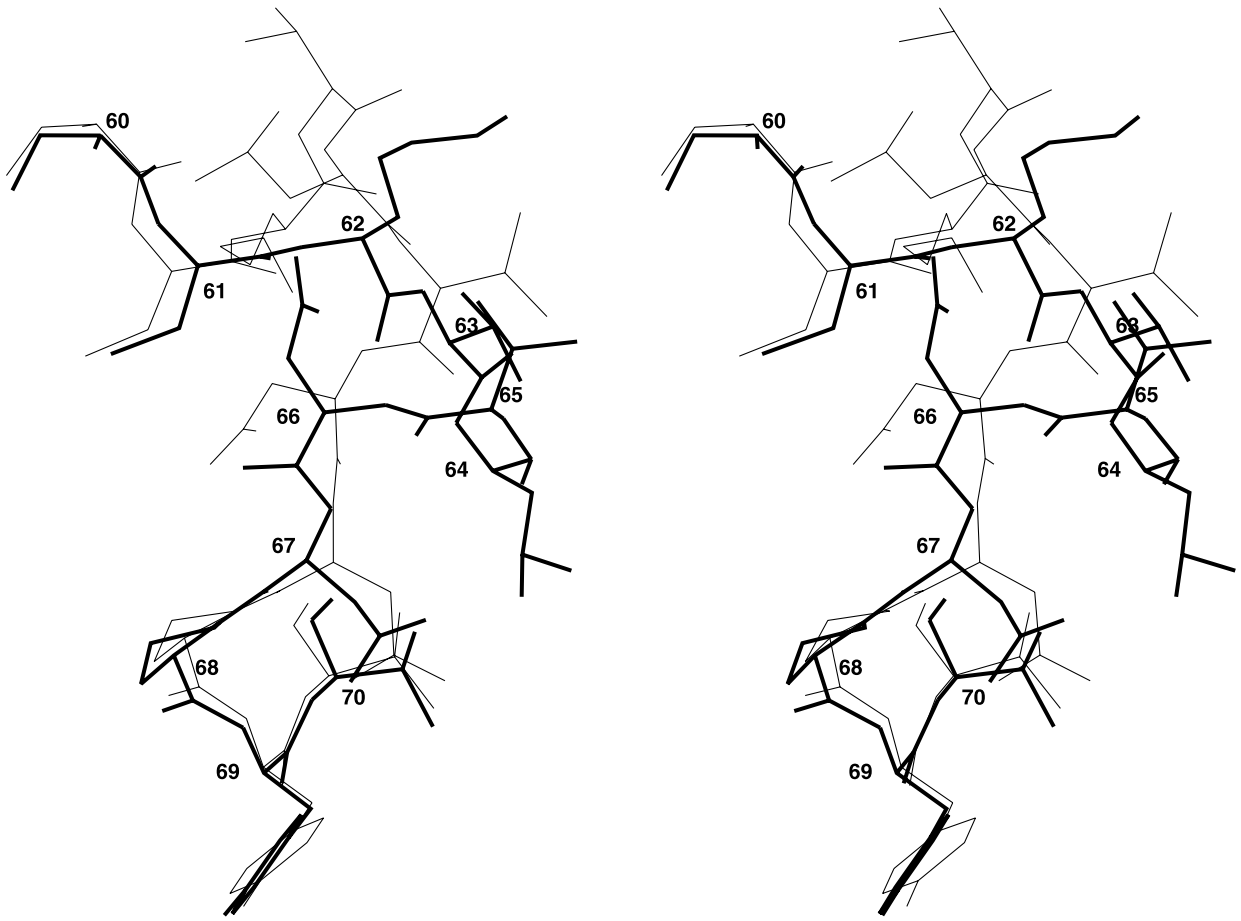

Figure 3. A stereo-view of the superposition of the surface loop residues in the triple mutant (thick lines) and the orthorhombic form of the wild-type (thin lines, PDB-id code: 1UNE). Residues 62–66 adopt a different conformation compared to the orthorhombic form.

at the interface. Earlier analyses on the kinetic effects of the single lysine substitutions[17] and deletions[18] in bovine PLA2 suggested that there is an incremental role for these lysine residues in the anionic interface preference of bovine PLA2. Recent biochemical studies also showed that lysine to methionine substitution induces a structural change that promotes the binding of PLA2 to the interface, as well as the substrate binding to the enzyme at the interface.[19] Further analyses suggested that the charge compensation of these positively charged residues contribute to the k^*_{cat} activation.

However, the location of these positively charged residues differ from the i-face that is involved in interfacial binding. Questions have been raised as to whether and how these distantly located structural features work together to facilitate the catalytic process and the recognition at the interface. Previous spectroscopic studies have shown that lysine-to-methionine mutations led to perturbation in the environment of Trp3 side-chain on the i-face.[20] Such "structural reciprocity" between distal regions has been considered one of the important structural features of pancreatic PLA2.[2] The results of the present study further suggest that the structural reciprocity could also exist between the k^*_{cat} allosteric site and the surface loop residues, which in turn affects binding of the second calcium ion. Taken together, our results further demonstrate the intricate structural properties that are inter-related and are responsible for various functional properties of PLA2.

The MPD molecule

The occurrence of the MPD molecule, the organic solvent used for crystallizing the enzyme, in the crystal structure is not uncommon.[21–23] Normally in the crystal structure of the PLA2–inhibitor complex, the inhibitor molecule occupies this site. There is good evidence that a MPD molecule is found in the active site of bovine pancreatic PLA2.[21,22] In the present structure, we also find clear electron density for the MPD molecule in the active site. One of the hydroxyl groups of the MPD molecule is hydrogen bonded to two water molecules, out of which one is a natural ligand for the catalytic calcium ion. The other hydroxyl group is involved in the hydrogen bonding with the backbone carbonyl of Phe22 and also with a water molecule.

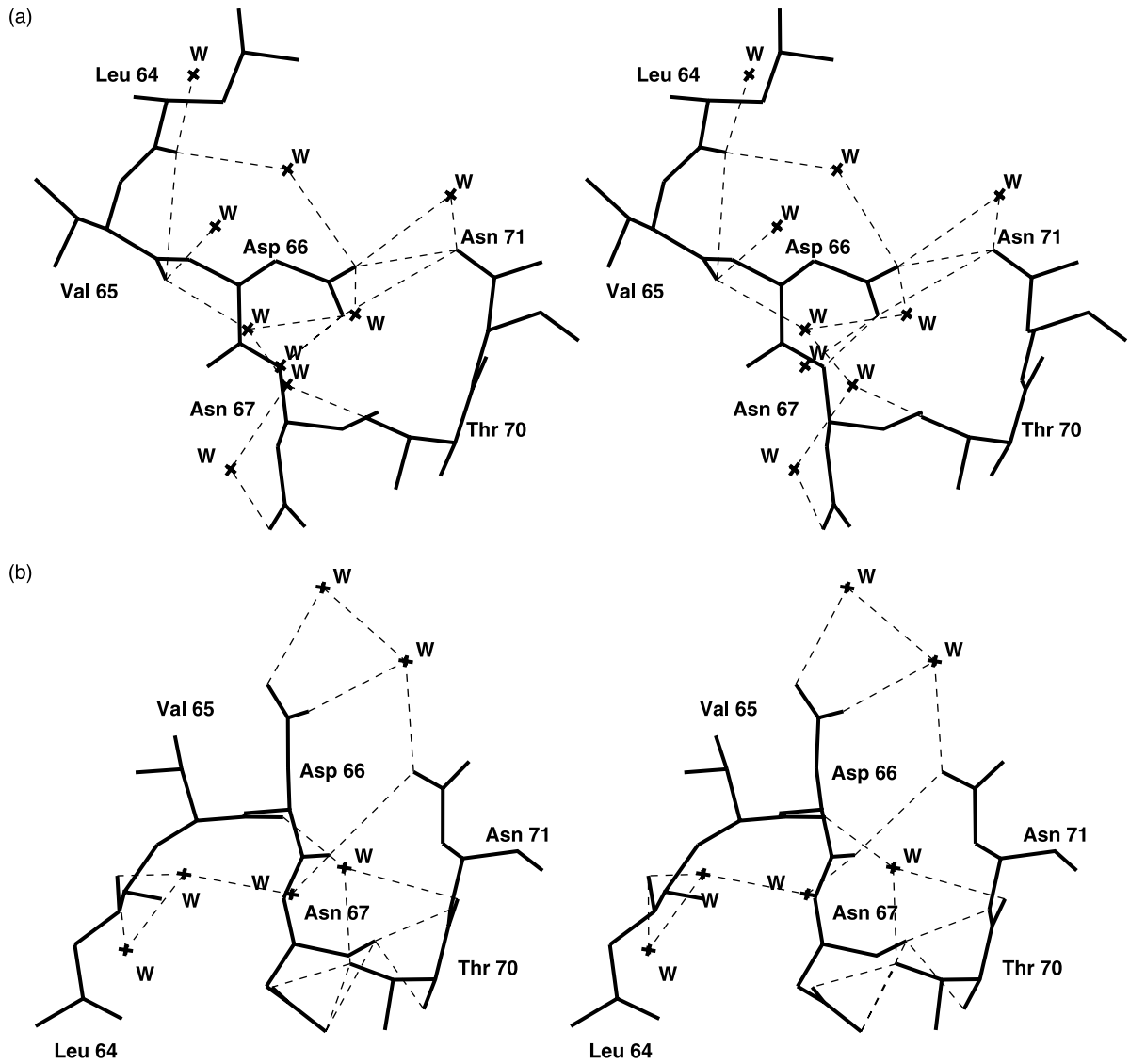

Figure 4. An overview of the hydrogen-bonding pattern involving the surface loop residues, water molecules and the residue Asn71 observed in the orthorhombic form[10] (a) and in the present triple mutant structure (b).

Conclusions

The three-dimensional structure of the triple mutant K56,120,121M of the recombinant bovine pancreatic PLA2 has been determined at 1.9 Å resolution and its overall fold is similar to that of the trigonal and the orthorhombic forms of WT PLA2 structures. A remarkable difference is that unlike other bovine pancreatic PLA2 structures, the residues 62–66 in the surface loop are well ordered and this loop adopts a different conformation. In addition, the present triple mutant structure reveals the presence of a second calcium ion, which is observed for the first time in bovine pancreatic PLA2. The structural change of the surface loop could be due to the conformational change of the residue Asn71 induced by the secondary calcium ion. The structural reciprocity between the k^*_{cat} allosteric site and the surface loop at the i-face represents a newly identified structural property of PLA2.

Materials and Methods

Site-directed mutagenesis and protein purification

Site-directed mutagenesis was conducted using the Quickchange method (Stratagene) with pET25(m)-pro-PLA2 as DNA template. The triple mutant K56,120,121M was generated by using pET25(m)-pro-PLA2-K56M single mutant as DNA template, and mutagenesis reactions for the single and triple mutants were carried out with oligonucleotides in complementary sets: 5′-AACACAAGAATCTTGATATGATGAACTGTT-AAGCTTCTG-3′ (K120, 121 to M), and 5′-TGCTATAAA-CAAGCTATGAAACTTGATAGCTGC-3′ (K56 to M). The recombinant PLA2 mutant was expressed in *Escherichia coli* BL 21 (DE3) pLys S strain (Novagen) in

the form of inclusion bodies, which was refolded and purified as described previously.[24]

Crystallization and data collection

Protein samples of the triple mutant were dissolved in 50 mM Tris buffer (pH 7.2), containing 5 mM $CaCl_2$, to a final protein concentration of 17–20 mg ml^{-1}. Crystals that could diffract to 1.9 Å resolution were obtained at room temperature (293 K) using hanging drop vapor diffusion method and the crystals grew within a week. The crystallization droplet contained 5 µl protein solution (17–20 mg ml^{-1}) in 50 mM Tris buffer, pH 7.2, and 2 µl of 2-methyl-2,4-pentane diol (MPD) (60%) and the reservoir contained 70% MPD.

Complete X-ray intensity data were collected from a single crystal with dimensions $0.20 \times 0.30 \times 0.30$ mm^3 at room temperature using a 300 mm Mar Research imaging plate detector mounted on a Rigaku rotating anode generator operated at 40 kV, 56 mA equipped with a Cu Kα target. The detector was placed 100 mm away from the crystal. An oscillation angle of 1° was used to collect the data. The data were integrated, scaled and reduced to 1.9 Å resolution with DENZO and SCALEPACK.[25,26] A total of 40,817 observations were measured which gave 8880 unique reflections with an R_{merge} of 7.5%.

Structure solution, model building and refinement

The present structure is P2, monoclinic system. The structure was solved by the molecular replacement calculations using the program AMoRe.[27] The atomic coordinates of the orthorhombic form of the recombinant PLA2 (PDB-id code: 1UNE) were used as the starting model, since it has the highest resolution among all the structures solved todate.[13] To monitor the progress of the refinement and to check the quality of the model, a total of 743 reflections (8% of the total reflections) were used to calculate the R_{free}.[28] Initially 30 cycles of rigid body refinement were carried out, followed by 50 cycles of positional refinement. Without the mutated residues Met56, Met120 and Met121, the *R*-value dropped to 38.5% ($R_{free} = 39.2\%$) for all the reflections in the resolution range 14.2–1.9 Å. The methionine residues were then inserted and fitted into the electron density map. Then the model was subjected to simulated annealing by employing a slow-cooling protocol, starting from 1500 K and cooling to 300 K in steps of 25 K at 0.5 fs, followed by 200 cycles of positional refinement which dropped the *R*-value to 31.3% ($R_{free} = 33.1\%$). To reduce the model bias, density modification protocol (solvent flipping and solvent flattening) was carried out without the surface loop residues. The resultant electron density map was clear enough to fit the surface loop residues. The difference maps also revealed the electron density for the functionally important calcium ion (primary calcium ion) in the active site. Surprisingly, in addition to the primary calcium ion, one more strong peak was found near the N-terminal region (peak height = 6σ). Since no other metal ions (except $CaCl_2$ in the crystallization buffer) were used during purification and crystallization, we interpreted the strong peak as an ion (either calcium ion or chloride ion). We have also seen six ligands with reasonable coordination distance (<2.6 Å) (three protein ligands and three water molecules) around the strong peak. On the basis of the neighboring ligand properties and from the earlier crystal structure evidences (see Results and Discussion for details), we interpreted this peak as calcium ion. The calcium–ligand distances were not restrained during the course of the refinement. At this stage individual *B*-factor refinement was started. During the progress of the refinement, additional water molecules were picked and included in the refinement. Omit maps (omitting 20 residues at a time) were calculated and used to correct or check the final protein model. In all, 125 water molecules were included in the refinement and the final *R*-value was 19.6% ($R_{free} = 25.9\%$). Bulk solvent correction was applied to all data during the refinement. The structure was refined in the resolution range (14.2–1.9 Å) without any sigma cutoff (including all the reflections) using the maximum likelihood (target function) and slow cooling (torsion angle dynamics) protocols as implemented in the refinement package CNS (1.0).[29] All the refinement calculations were performed using CNS (1.0). The molecular modeling program FRODO[30] was used to fit the protein model into the electron density. The atomic coordinates and the structural factors have been deposited in the PDB[11] with the accession codes 1GH4 and R1GH4SF, respectively.

Acknowledgements

The intensity data were collected at the X-ray facility for structural biology at the Molecular Biophysics Unit, Indian Institute of Science, Bangalore, India, supported by the Department of Science and Technology (DST) and the Department of Biotechnology (DBT), India. In addition, facilities at the Supercomputer Education and Research Centre, the Interactive Graphics Molecular Modeling Facility and the Distributed Information Centre are gratefully acknowledged. The work from Dr Tsai's lab was supported by NIH grant GM 41788.

References

1. Waite, M. (1987). Handbook of Lipid Research, vol. 5, Plenum Press, New York.
2. Berg, O. G., Gelb, M., Tsai, M.-D. & Jain, M. K. (2001). Interfacial enzymology: the phospholipase A_2 paradigm. *Chem. Rev.* **101**, 2613–2653.
3. Sekar, K., Eswaramoorthy, S., Jain, M. K. & Sundaralingam, M. (1997). Crystal structure of the complex bovine pancreatic phospholipase A_2 with the inhibitor 1-hex decyl-3-(trifluro ethyl)-*sn*-glycero-2-phosphomethanol. *Biochemistry*, **36**, 14186–14191.
4. Sekar, K., Kumar, A., Liu, X., Tsai, M.-D., Gelb, M. H. & Sundaralingam, M. (1998). Structure of the complex of bovine pancreatic phospholipase A_2 with a transition state anologue. *Acta Crystallog. sect. D*, **54**, 334–341.
5. Sekar, K., Sekharudu, C., Tsai, M.-D. & Sundaralingam, M. (1998). 1.72 Å resolution refinement of the trigonal form of bovine pancreatic phospholipase A_2. *Acta Crystallog. sect. D*, **54**, 342–346.
6. Sekar, K., Biswas, R., Li, Y., M, D. & Sundaralingam, M. (1999). Structures of the catalytic site mutants D99A and H48Q and the calcium loop mutant D49E

of phospholipase A_2. *Acta Crytallog. sect. D*, **55**, 443–447.
7. Dijkstra, B. W., Renetseder, R., Kalk, K. H., Hol, W. G. J. & Drenth, J. (1983). Structure of porcine pancreatic phospholipase A_2 at 2.6 Å resolution and comparison with bovine pancreatic phospholipase A_2. *J. Mol. Biol.* **168**, 163–179.
8. Thunnissen, M. M. G. M., Franken, P. A., de Hass, G. H., Drenth, J., Kalk, K. H., Verheij, H. M. & Dijkstra, B. W. (1993). Crystal structure of a porcine phospholipase A_2 mutant. A large conformational change caused by the F63V point mutation. *J. Mol. Biol.* **232**, 839–855.
9. Laskowski, R. A., MacArthur, M. W., Moss, D. S. & Thornton, J. M. (1993). PROCHECK: a program to check the stereochemical quality of protein structures. *J. Appl. Crystallog.* **26**, 283–291.
10. Sekar, K. & Sundaralingam, M. (1999). High resolution refinement of orthorhombic bovine pancreatic phospholipase A_2. *Acta Crystallog. sect. D*, **55**, 46–50.
11. Bernstein, F. C., Koetzle, T. F., Williams, G. J. B., Meyer, E. F., Jr, Brice, M. D., Rodgers, J. R. *et al.* (1977). The Protein Data Bank: a computer based archival file for macromolecular structures. *J. Mol. Biol.* **112**, 535–542.
12. Slotboom, A. J., Jansen, E. H. J. M., Vlijm, J., Patuus, J., de Araujo, P. S. & de Hass, G. H. (1978). Ca^{2+} binding to porcine phospholipase A_2 and its function in enzyme–lipid interaction. *Biochemistry*, **17**, 4593–4600.
13. Anderson, T., Drakenberg, T., Forsen, S., Wieloch, T. & Lindstorm, M. (1981). Calcium binding to porcine pancreatic phospholipase A_2 studied by ^{43}Ca NMR. *FEBS Letters*, **123**, 115–117.
14. van den Bergh, C. J., Bekkars, A. C., Verheij, H. M. & de Haas, G. H. (1989). Glutamic acid 71 and aspartic acid 66 control the binding of the second calcium ion in porcine phospholipase A_2. *Eur. J. Biochem.* **182**, 307–313.
15. Donne-Op den Kelder, G. M., de Haas, G. H. & Egmond, M. R. (1983). Localization of the second calcium ion binding site in porcine and equine phospholipase A_2. *Biochemistry*, **22**, 2470–2478.
16. Sekar, K., Yu, B.-Z., Rogers, J., Lutton, J., Liu, X., Chen, X. *et al.* (1997). Phospholipase A_2 engineering. Structural and functional roles of the highly conserved active site residue aspartate-99. *Biochemistry*, **36**, 3101–3114.
17. Rogers, J., Yu, B. Z., Tsai, M. D., Berg, O. G. & Jain, M. K. (1998). Cationic residues 53 and 56 control the anion-induced interfacial k^*_{cat} activation of pancreatic phospholipase A_2. *Biochemistry*, **37**, 9549–9556.
18. Huang, B., Yu, B. Z., Rogers, J., Byeon, I. J., Sekar, K., Chen, X. *et al.* (1996). Phospholipase A_2 engineering. Deletion of the C-terminus segment changes substrate specificity and uncouples calcium and substrate binding at the Zwitterionic interface. *Biochemistry*, **36**, 12164–12174.
19. Yu, B.-Z., Poi, M. J., Ramagopal, U. A., Jain, R., Ramakumar, S., Berg, O. G. *et al.* (2000). Structural basis of the anionic interface preference and k^*_{cat} activation of pancreatic phospholipase A_2. *Biochemistry*, **39**, 12312–12323.
20. Berg, O. G., Rogers, J., Yu, B.-Z., Yao, J., Romsted, L. S. & Jain, M. K. (1997). Thermodynamic and kinetic basis for interfacial activation: resolution of binding and allosteric effects of pancreatic phospholipase A_2. *Biochemistry*, **36**, 14512–14530.
21. Dijkstra, B. W., Kalk, K. H., Hol, W. G. J. & Drenth, J. (1981). Structure of bovine pancreatic phospholipase A_2 at 1.7 Å resolution. *J. Mol. Biol.* **147**, 97–123.
22. Steiner, R. A., Rozeboom, H. J., de Vries, A., Kalk, K. H., Murshudov, G. N., Wilson, K. S. & Dijkstra, B. W. (2001). X-ray structure of bovine pancreatic phospholipase A_2 at atomic resolution. *Acta Crystallog. sect. D*, **57**, 516–526.
23. Weiss, M. S., Palm, G. J. & Hilgenfeld, R. (2000). Crystallization, structure solution and refinement of hen egg-white lysozyme at pH 8.0 in the presence of MPD. *Acta Crystallog. sect. D*, **56**, 952–958.
24. Deng, T., Noel, J. P. & Tsai, M.-D. (1990). A novel expression vector for high-level synthesis and secretion of foreign proteins in *E. coli*: over production of bovine pancreatic phospholipase A_2. *Gene*, **93**, 229–234.
25. Otwinowski, W. (1993). *Proceedings of the CCP4 study weekend*, Daresbury Laboratory Warrington, UK pp. 56–62.
26. Minor, W. (1993). XDISPLAYF Program, Purdue University.
27. Navaza, J. (1994). AMoRe: an automated package for molecular replacement. *Acta Crystallog. sect. A*, **50**, 157–163.
28. Brunger, A. T. (1992). Free *R*-value: a novel statistical quantity for assessing the accuracy of crystal structures. *Nature (London)*, **355**, 472–474.
29. Brunger, A. T., Adams, P. D., Clore, G. M., DeLano, W. L., Gros, P., Kunstleve, G. R. G. *et al.* (1998). Crystallography and NMR system: a new software suite for macromolecular structure determination. *Acta Crytallog. sect. D*, **54**, 905–921.
30. Jones, T. A. (1985). Diffraction methods for biological macromolecules. Interactive graphics FRODO. *Methods Enzymol.* **115**, 157–171.

Edited by Sir A. Klug

(Received 17 July 2002; received in revised form 2 October 2002; accepted 8 October 2002)